



Available online at <http://scik.org>

Commun. Math. Biol. Neurosci. 2023, 2023:88

<https://doi.org/10.28919/cmbn/8092>

ISSN: 2052-2541

STABILITY ANALYSIS OF *SLIVR* COVID-19 EPIDEMIC MODEL WITH QUARANTINE POLICY

YOUSRA HAJRI, EL MEHDI FARAH*, AMINA ALLALI, SAIDA AMINE

Laboratory of Mathematics, Computer Science and Applications, Faculty of Sciences and Technics, Hassan II
University of Casablanca, PO Box 146, Mohammedia 20650, Morocco

Copyright © 2023 the author(s). This is an open access article distributed under the Creative Commons Attribution License, which permits unrestricted use, distribution, and reproduction in any medium, provided the original work is properly cited.

Abstract. In this paper, we present a mathematical model illustrating the dynamics of the COVID-19 disease with vaccination and quarantine strategies. The presented model contains five equations that describe the interaction between individuals who are susceptible, exposed, infected, vaccinated, and recovered. We start the study by verifying the positivity and boundedness of solutions. The existence and the stability of both disease-free equilibrium and endemic equilibrium are proved. Finally, numerical simulations are performed to demonstrate the behavior of the infection over time and to say the influence of quarantine and vaccination on both the COVID-19 dynamics and the basic reproduction number $mathcal{R}_0$ for controlling the disease's spread.

Keywords: COVID-19; epidemic model; stability; quarantine policy.

2020 AMS Subject Classification: 92C60.

1. INTRODUCTION

SARS-CoV-2, a coronavirus discovered in 2019, has produced a respiratory disease pandemic known as COVID-19. The virus spreads between people through direct contact or via contaminated surfaces. This disease is currently spreading rapidly in many countries, and the global number of COVID-19 cases is rapidly increasing.

*Corresponding author

E-mail address: elmehdi.farah.ed@gmail.com

Received July 05, 2023

Mathematical modelling in epidemiology is a source of knowledge for understanding the spread of an disease and an effective tool for controlling and predicting the dynamics of diseases such as Cancer [1], VIH [2], influenza [3], Tuberculosis [4], HBV [5], COVID-19 [11, 12, 13] and the co-infection of COVID-19 and HBV [6], other researchers are interested in modeling multi-strain diseases [7, 8, 10, 9]. Many active studies are currently being conducted to investigate various epidemic models applied to the spread of COVID-19 by scientists all over the world. Ian et al. [14] developed a susceptible-infected-removed (SIR) model that provides a theoretical framework to investigate the time evolution of different populations and monitor diverse significant parameters for the spread of the disease COVID-19 in various communities. In addition, the SARS-COV-2 virus has a long incubation period, which refers to the time between being exposed to the virus and developing symptoms. The average incubation period is 6 days, with recorded variations ranging from 2 to 27 days [15]. As a result, many earlier studies considered a new compartment to the classic SIR in model to account for the exposed population. An SLIR model was implimented by Shaobo et al. [19], to analyse the spread of COVID-19 in Hubei province. Additionally many mathematical models were constructed to study the outbreak of COVID-19 in many countries [16, 17, 18].

Countries worldwide have implemented strict and adequate precautions to prevent and control the spread of COVID-19, including early detection approaches and social distancing [20] to limit contact between individuals as much as possible, as well as medical treatment, to reduce the number of infected citizens. Vaccination is a crucial strategy in fighting against many previously infected diseases. Recently, authors in [21] constructed a *SLIR* model by considering vaccination and isolation factors as model parameters. Moreover, Amouch et al. [22] proposed a new epidemiological mathematical model for the spread of the COVID-19 disease with a special focus on the transmissibility of individuals with severe symptoms, mild symptoms, and asymptomatic symptoms and take into consideration the vaccination of a portion of susceptible individuals. More recently, a COVID-19 vaccine epidemic model has been tackled [23]. In this work, we continue the investigation of the effect of vaccination by taking into account the effect of quarantine measures on SLIVR COVID-19 epidemic model presented in [23]. Therefore, the

SLIVR COVID-19 epidemic model is formulated as follows

$$(1) \quad \begin{cases} \frac{d\mathcal{S}(t)}{dt} = \Lambda - \beta(1-\rho)(\mathcal{S}(t) + \alpha\mathcal{L}(t))\frac{\mathcal{S}(t)}{N} - (r_v + d)\mathcal{S}(t) + w_v\mathcal{V}(t) + l_m\mathcal{R}(t), \\ \frac{d\mathcal{L}(t)}{dt} = \beta(1-\rho)(\mathcal{S}(t) + \alpha\mathcal{L}(t))\frac{\mathcal{S}(t)}{N} - (d + r_s)\mathcal{L}(t), \\ \frac{d\mathcal{I}(t)}{dt} = r_s\mathcal{L}(t) - (d + d_0 + r_c)\mathcal{I}(t), \\ \frac{d\mathcal{V}(t)}{dt} = r_v\mathcal{S}(t) - (d + w_v)\mathcal{V}(t), \\ \frac{d\mathcal{R}(t)}{dt} = r_c\mathcal{I}(t) - (d + l_m)\mathcal{R}(t), \end{cases}$$

with

$$(2) \quad \mathcal{S}(0) \geq 0, \mathcal{L}(0) \geq 0, \mathcal{I}(0) \geq 0, \mathcal{V}(0) \geq 0, \mathcal{R}(0) \geq 0.$$

This model includes six variables: susceptible individuals (\mathcal{S}), the population that can make contact with the infection, the exposed individuals (\mathcal{L}), the population exposed to the virus but without developing clinical symptoms. The infectious individuals (\mathcal{I}), the population with fully developed corona-virus symptoms. The vaccinated individuals (\mathcal{V}), and finally removed individuals (\mathcal{R}). All model parameters are assumed to be positive and are described as follows: Λ denotes the population recruitment rate and d is natural mortality in all compartments. β represent the effective contact rate, α represents relative transmissibility rate. r_s represents rate of infection development with symptoms, d_0 is death rate due to infection and r_c is rate of recovery from infection. r_v denote vaccination rate, w_v is vaccine waning rate and l_m is loss of disease acquired immunity. The parameter ρ represent the efficiency of quarantine in reducing the latent and infected individuals. The flowchart of our model is illustrated in Fig. 1.

The current work is divided into different sections. In the following section, we will demonstrate the existence, the positivity and boundedness results. In Section 3, we will establish both the local and global stability of both equilibrium. In Section 4, we will present some numerical simulations to verify the theoretical results. The conclusion is stated in Section 5.

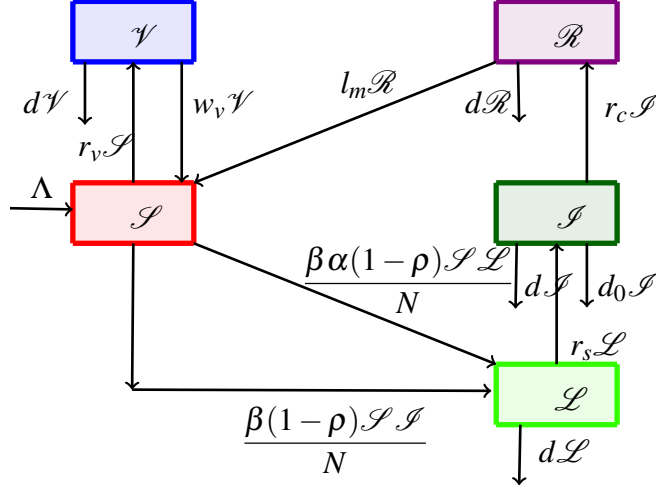


FIGURE 1. The diagram of the COVID-19 model.

2. THE PROBLEM WELLPOSEDNESS AND STEADY STATES

In this section, we will prove that the system is biologically meaningful and mathematically well posed. To do this, it is required to prove that the solutions of the system of ordinary differential equation (1) are positive and bounded for all time.

2.1. Existence, positivity and boundedness.

Proposition 2.1. *For all non-negative initial condition, the solutions of the system (1) exist, non-negative and remain bounded for all $t > 0$. Moreover,*

$$\lim_{t \rightarrow +\infty} N(t) \leq \frac{\Lambda}{d}.$$

Proof. In order to prove the positivity result, we will show that any solution starting from non-negative orthant \mathbb{R}_+^5 remains there forever.

Let

$$(3) T = \sup\{\tau > 0 : \forall t \in [0, \tau] \text{ such that } \mathcal{S}(t) \geq 0, \mathcal{L}(t) \geq 0, \mathcal{I}(t) \geq 0, \mathcal{V}(t) \geq 0, \mathcal{R}(t) \geq 0\}$$

Let us now show that $T = +\infty$. Suppose the contrary. By continuity of solutions, we have $\mathcal{S}(T) = 0$ or $\mathcal{L}(T) = 0$ or $\mathcal{I}(T) = 0$ or $\mathcal{V}(T) = 0$ or $\mathcal{R}(T) = 0$.

- If $\mathcal{S}(T) = 0$ before the other variables $\mathcal{L}, \mathcal{I}, \mathcal{V}, \mathcal{R}$, becomes zero. Hence,

$$\frac{d\mathcal{S}}{dt} = \lim_{t \rightarrow T^-} \frac{\mathcal{S}(T) - \mathcal{S}(t)}{T - t} = \lim_{t \rightarrow T^-} \frac{-\mathcal{S}(t)}{T - t} \leq 0.$$

Using the first equation of system (1), we obtain

$$\begin{aligned} \frac{d\mathcal{S}(T)}{dt} &= \Lambda - \beta(1 - \rho)(\mathcal{I}(T) + \alpha\mathcal{L}(T))\frac{\mathcal{S}(T)}{N} - (r_v + d)\mathcal{S}(T) + w_v\mathcal{V}(T) + l_m\mathcal{R}(T), \\ &= \Lambda + w_v\mathcal{V}(T) + l_m\mathcal{R}(T), \end{aligned}$$

So, $\frac{d\mathcal{S}(T)}{dt} > 0$. Which presents a contradiction.

- If $\mathcal{L}(T) = 0$ before the other variables $\mathcal{S}, \mathcal{I}, \mathcal{V}, \mathcal{R}$, becomes zero. Hence,

$$\frac{d\mathcal{L}}{dt} = \lim_{t \rightarrow T^-} \frac{\mathcal{L}(T) - \mathcal{L}(t)}{T - t} = \lim_{t \rightarrow T^-} \frac{-\mathcal{L}(t)}{T - t} \leq 0.$$

Using the first equation of system (1), we obtain

$$\begin{aligned} \frac{d\mathcal{L}(T)}{dt} &= \beta(1 - \rho)(\mathcal{I}(T) + \alpha\mathcal{L}(T))\frac{\mathcal{S}(T)}{N} - (d + r_s)\mathcal{L}(T), \\ &= \frac{\beta(1 - \rho)\mathcal{I}(T)\mathcal{S}(T)}{N}, \end{aligned}$$

So, $\frac{d\mathcal{L}(T)}{dt} > 0$. Which presents a contradiction. Similar proof for $\mathcal{I}(t), \mathcal{V}(t), \mathcal{R}(t)$.

Therefore, T could not be finite, which implies that $\mathcal{S}, \mathcal{L}, \mathcal{I}, \mathcal{V}$ and \mathcal{R} are all positive for all positive time. This proof the positivity of solutions.

To prove the subsequent part of Proposition (2.1), let the total population

$$N(t) = \mathcal{S}(t) + \mathcal{L}(t) + \mathcal{I}(t) + \mathcal{V}(t) + \mathcal{R}(t).$$

By adding equations involved in the system (1), we have

$$(4) \quad \begin{aligned} \frac{dN}{dt} &= \Lambda - dN - d_0\mathcal{I} \\ &\leq \Lambda - dN. \end{aligned}$$

By simple manipulation, we have

$$\begin{aligned} N(t) &\leq N(0)e^{-dt} + e^{-dt} \int_0^t \Lambda e^{-d\xi} d\xi \\ &\leq N(0)e^{-dt} + \frac{\Lambda}{d} (1 - e^{-dt}) \end{aligned}$$

Thus,

$$\lim_{t \rightarrow +\infty} N(t) \leq \frac{\Lambda}{d}$$

□

2.2. Invariant region.

Proposition 2.2. *The biological feasible region for the transmission dynamic of COVID-19 epidemic model (1) is given by $\Omega \subset \mathbf{R}_+^5$, where,*

$$\Omega = \left\{ (\mathcal{S}, \mathcal{L}, \mathcal{I}, \mathcal{V}, \mathcal{R}) \in \mathbf{R}_+^5 : \mathcal{S} + \mathcal{L} + \mathcal{I} + \mathcal{V} + \mathcal{R} \leq \frac{\Lambda}{d} \right\}.$$

Moreover, the closed region define by $\Omega \subset \mathbf{R}_+^5$ is positive invariant for the model (1) with nonnegative initial conditions in \mathbf{R}_+^5 .

Proof. As we know that

$$N(t) = \mathcal{S}(t) + \mathcal{L}(t) + \mathcal{I}(t) + \mathcal{V}(t) + \mathcal{R}(t),$$

then,

$$\begin{aligned} (5) \quad \frac{dN(t)}{dt} &= \Lambda - dN(t) - d_0 \mathcal{I} \\ &\leq \Lambda - dN(t), \end{aligned}$$

and

$$\frac{dN(t)}{dt} \leq 0 \text{ if } N(t) \geq \frac{\Lambda}{d} \text{ for } t \geq 0,$$

but the solution of (5) is

$$N(t) \leq N(0)e^{-dt} + \frac{\Lambda}{d} (1 - e^{-dt}).$$

Therefore, $N(t) \leq \frac{\Lambda}{d}$ if $N(0) \leq \frac{\Lambda}{d}$ as $t \rightarrow \infty$. On other hand $N(t) > \frac{\Lambda}{d}$ if $N(0) > \frac{\Lambda}{d}$ as $t \rightarrow \infty$.

Thus, the region Ω is positive invariant, and all the solutions trajectories are attracted in \mathbf{R}_+^5 □

3. ANALYSIS OF THE MODEL

In this section, we will first calculate the basic reproduction number \mathcal{R}_0 for The COVID-19 model (1). Next, we will present the steady states and finally we will demonstrate the local and global stability of all steady states.

3.1. The Basic Reproduction Number. Biologically, the basic reproduction number denoted \mathcal{R}_0 represents the average number of new infections generated by each infected person in a population where all individuals are susceptible to infection. We will use the next generation matrix to calculate the basic reproduction number \mathcal{R}_0 [24]. The necessary matrices denoted by F and Y are given by given by

$$F = \begin{pmatrix} \beta\alpha(1-\rho)\frac{\Lambda(d+w_v)}{N^0d(d+w_v+r_v)} & \beta(1-\rho)\frac{\Lambda(d+w_v)}{N^0d(d+w_v+r_v)} & 0 \\ 0 & 0 & 0 \\ 0 & 0 & 0 \end{pmatrix}$$

$$\text{and } Y = \begin{pmatrix} d+r_s & 0 & 0 \\ -r_s & d+d_0+r_c & 0 \\ 0 & 0 & d+w_v \end{pmatrix}.$$

$$\text{Since, } N^0 = \frac{\Lambda}{d}. \text{ Then, } F = \begin{pmatrix} \frac{\beta(1-\rho)\alpha(d+w_v)}{d+w_v+r_v} & \frac{\beta(1-\rho)(d+w_v)}{d+w_v+r_v} & 0 \\ 0 & 0 & 0 \\ 0 & 0 & 0 \end{pmatrix}$$

$$\text{and } Y = \begin{pmatrix} d+r_s & 0 & 0 \\ -r_s & d+d_0+r_c & 0 \\ 0 & 0 & d+w_v \end{pmatrix}.$$

Therefore,

$$FY^{-1} = \begin{pmatrix} \frac{\beta(1-\rho)\alpha(d+w_v)}{(d+r_s)(d+w_v+r_v)} + \frac{\beta(1-\rho)r_s(d+w_v)}{(d+r_s)(d+w_v+r_v)(d+d_0+r_c)} & \frac{\beta(1-\rho)(d+w_v)}{(d+w_v+r_v)(d+d_0+r_c)} & 0 \\ 0 & 0 & 0 \\ 0 & 0 & 0 \end{pmatrix}.$$

The basic reproduction number \mathcal{R}_0 is obtained as the spectral radius of FY^{-1} . Hence, we get the following expression of \mathcal{R}_0

$$\mathcal{R}_0 = \frac{\beta(1-\rho)(d+w_v)(r_s+\alpha(d+d_0+r_c))}{(d+r_s)(d+w_v+r_v)(d+d_0+r_c)},$$

$$\mathcal{R}_0 = \mathcal{R}_1 + \mathcal{R}_2,$$

$$\text{where } \mathcal{R}_1 = \frac{\beta(1-\rho)r_s(d+w_v)}{(d+r_s)(d+w_v+r_v)(d+d_0+r_c)} \text{ and } \mathcal{R}_2 = \frac{\beta(1-\rho)\alpha(d+w_v)}{(d+r_s)(d+w_v+r_v)}.$$

3.2. Steady states. In the next Theorem, the steady states of the the COVID-19 epidemic model (1) are given.

Theorem 3.1. -The COVID-19 epidemic model (1) has a disease free equilibrium defined by

$$\mathcal{P}_0 = (\mathcal{S}_0, \mathcal{L}_0, \mathcal{I}_0, \mathcal{V}_0, \mathcal{R}_0) = \left(\frac{\Lambda(d+w_v)}{d(d+w_v+r_v)}, 0, 0, \frac{\Lambda r_v}{d(d+w_v+r_v)}, 0 \right).$$

-If $\mathcal{R}_0 > 1$, then the COVID-19 epidemic model (1) has endemic equilibrium points given by

$$\mathcal{P}^* = (\mathcal{S}^*, \mathcal{L}^*, \mathcal{I}^*, \mathcal{V}^*, \mathcal{R}^*), \text{ where}$$

$$(6) \quad \left\{ \begin{array}{l} \mathcal{S}^* = \frac{\Lambda(d+w_v)M_2}{(d+w_v+r_v)[(\mathcal{R}_0-1)M_1+dM_2]}, \\ \mathcal{L}^* = \frac{\Lambda(d+l_m)(d+d_0+r_c)(\mathcal{R}_0-1)}{(\mathcal{R}_0-1)M_1+dM_2}, \\ \mathcal{I}^* = \frac{r_s\Lambda(d+l_m)(\mathcal{R}_0-1)}{(\mathcal{R}_0-1)M_1+dM_2}, \\ \mathcal{V}^* = \frac{\Lambda r_v M_2}{(d+w_v+r_v)((\mathcal{R}_0-1)M_1+dM_2)}, \\ \mathcal{R}^* = \frac{r_s r_c \Lambda (\mathcal{R}_0-1)}{(\mathcal{R}_0-1)M_1+dM_2}, \end{array} \right.$$

where

$$(7) \quad \begin{aligned} M_1 &= d(d+l_m)(d+r_c) + dr_s(d+r_c+l_m) + d_0(d+r_s)(d+l_m), \\ M_2 &= (d+l_m)(d+d_0+r_c) + r_s(d+r_c+l_m). \end{aligned}$$

3.3. Local Stability.

Theorem 3.2. The disease-free equilibrium, \mathcal{P}_0 is locally asymptotically stable if $\mathcal{R}_0 < 1$ and else unstable.

Proof. The Jacobian of model (1) at disease-free equilibrium,

$$\mathcal{P}_0 = \left(\frac{\Lambda(d+w_v)}{d(d+w_v+r_v)}, 0, 0, \frac{\Lambda r_v}{d(d+w_v+r_v)}, 0 \right) \text{ is,}$$

$$J(\mathcal{P}_0) = \begin{pmatrix} -d-r_v & -\frac{\beta(1-\rho)\alpha(d+w_v)}{d+w_v+r_v} & -\frac{\beta(1-\rho)(d+w_v)}{d+w_v+r_v} & w_v & l_m \\ 0 & -r_s-d+\frac{\beta(1-\rho)\alpha(d+w_v)}{d+w_v+r_v} & \frac{\beta(1-\rho)(d+w_v)}{d+w_v+r_v} & 0 & 0 \\ 0 & r_s & -d-d_0-r_c & 0 & 0 \\ r_v & 0 & 0 & 0 & -d-w_v \\ 0 & 0 & r_c & 0 & -l_m-d \end{pmatrix},$$

and the corresponding characteristic polynomial is

$$P(\xi) = (-\xi - l_m - d)(\xi + d)(\xi + d + w_v + r_v)(a_2\xi^2 + a_1\xi + a_0),$$

where

$$a_2 = 1,$$

$$a_1 = d + d_0 + r_c + (r_s + d)(1 - \mathcal{R}_2),$$

$$a_0 = (r_s + d)(d + d_0 + r_c)(d + w_v + r_v)(1 - \mathcal{R}_0).$$

When $\mathcal{R}_0 < 1$, the coefficients a_0 and a_1 are positive. By Routh-Hurwitz stability criteria, the disease-free equilibrium is locally asymptotically stable in Ω . \square

Theorem 3.3. *The endemic equilibrium \mathcal{P}^* is locally asymptotically stable when $\mathcal{R}_0 > 1$. Moreover, \mathcal{P}^* is otherwise unstable.*

Proof. The Jacobian of system (1) at $\mathcal{P}^* = (\mathcal{I}^*, \mathcal{L}^*, \mathcal{I}^*, \mathcal{V}^*, \mathcal{R}^*)$ is

$$J(\mathcal{P}^*) = \begin{pmatrix} -p_{11} & -p_{12} & -p_{13} & w_v & l_m \\ -p_{21} & -p_{22} & p_{23} & 0 & 0 \\ 0 & r_s & -p_{33} & 0 & 0 \\ r_v & 0 & 0 & -p_{44} & 0 \\ 0 & 0 & r_c & 0 & -p_{55} \end{pmatrix}$$

where

$$p_{11} = d + r_v + \lambda, \quad p_{12} = \beta(1-\rho)\alpha \frac{d\mathcal{I}_0}{\Lambda\mathcal{R}_0},$$

$$p_{13} = \beta(1-\rho)\frac{d\mathcal{I}_0}{\Lambda\mathcal{R}_0}, \quad p_{21} = \lambda, \quad p_{22} = d + r_s - \beta(1-\rho)\alpha \frac{d\mathcal{I}_0}{\Lambda\mathcal{R}_0},$$

$$p_{23} = \beta(1 - \rho) \frac{d\mathcal{S}_0}{\Lambda\mathcal{R}_0}, \quad p_{33} = d + d_0 + r_c, \quad p_{44} = d + w_v, \quad p_{55} = d + l_m.$$

The corresponding characteristics equation is given by

$$P(\zeta) = \zeta^5 + b_4\zeta^4 + b_3\zeta^3 + b_2\zeta^2 + b_1\zeta + b_0,$$

where

$$b_4 = \frac{\Lambda(d + r_s)(d + l_m)(d + d_0 + r_c)(\mathcal{R}_0 - 1)}{dM_2\mathcal{S}_0} + (d + r_s) \left(1 - \frac{R_2}{\mathcal{R}_0}\right) + (d + d_0 + r_c),$$

$$b_3 = p_{12}p_{21} + p_{33}p_{44} + (p_{33} + p_{44})p_{55} + p_{22}(p_{33} + p_{44} + p_{55}) \\ + p_{11}(p_{22} + p_{33} + p_{44} + p_{55}) - (r_s p_{23} + w_v r_v),$$

$$b_2 = r_s p_{13}p_{21} + p_{22}p_{33}(p_{44} + p_{55}) + p_{44}p_{55}(p_{11} + p_{22}) + p_{12}p_{21}(p_{33} + p_{44} + p_{55}) \\ + p_{11}(p_{33}p_{44} + (p_{33} + p_{44})p_{55} + p_{22}(p_{33} + p_{44} + p_{55})) - r_s p_{23}(p_{11} + p_{44} + p_{55}) \\ - w_v r_v(p_{22} + p_{33} + p_{55}),$$

$$b_1 = p_{33}p_{44}p_{55}(p_{11} + p_{22}) + p_{11}p_{55}(p_{22}p_{33} + (p_{22} + p_{33})p_{44}) \\ + p_{21}(r_s p_{13}(p_{44} + p_{55}) + p_{12}(p_{33}p_{44} + p_{55}(p_{33} + p_{44}))) + r_s w_v r_v p_{23}, \\ - r_s(p_{23}p_{44}p_{55} + p_{11}p_{23}(p_{44} + p_{55}) + l_m r_c p_{21}) - w_v r_v(p_{22}p_{33} - (p_{22} + p_{33})p_{55}) \\ b_0 = \frac{(d + l_m)(d + w_v)(d + r_s)(d + d_0 + r_c)M_1(\mathcal{R}_0 - 1)}{dM_2\mathcal{S}_0}.$$

The coefficients b_4, b_3, b_2, b_1, b_0 are positive if $\mathcal{R}_0 > 1$.

It is obvious to show that the necessary conditions of Routh-Hurwitz stability criteria for degree five polynomial, $b_4 b_3 b_2 > b_2^2 + b_4^2 b_1$ and $(b_4 b_1 - b_0)(b_4 b_3 b_2 - b_2^2 - b_4^2 b_1) > b_0(b_4 b_3 - b_2)^2 + b_1 b_0^2$ holds.

Therefore, the P^* is locally asymptotically stable in Ω . □

3.4. Global stability. The following Theorem investigates the global dynamics of disease-free equilibrium, \mathcal{P}_0 , of the COVID-19 epidemic model described in (1).

Theorem 3.4. *The disease-free equilibrium \mathcal{P}_0 is global asymptotically stable if $\mathcal{R}_0 < 1$, otherwise unstable.*

Proof. Consider the Lyapunov function given by

$$\mathcal{F}_0(\mathcal{L}, \mathcal{I}) = \mathcal{L} + g\mathcal{I}, \text{ where } g = \frac{\beta(1-\rho)(d+w_v)}{(d+w_v+r_v)(d+d_0+r_c)}.$$

Hence, the Lyapunov derivative is

$$\begin{aligned} \frac{d\mathcal{F}_0}{dt} &= \frac{d\mathcal{L}}{dt} + g\frac{d\mathcal{I}}{dt} \\ &= \left[\beta(1-\rho)(\mathcal{I} + \alpha\mathcal{L})\frac{\mathcal{I}}{N} - (d+r_s)\mathcal{L} \right] + g[r_s\mathcal{L} - (d+d_0+r_c)\mathcal{I}], \end{aligned}$$

Since,

$$\mathcal{I}(t) \leq \mathcal{I}_0 = \frac{\Lambda(d+w_v)}{d(d+w_v+r_v)} \text{ and } N(t) \leq \frac{\Lambda}{d} \text{ then } \frac{\mathcal{I}(t)}{N(t)} \leq \frac{d+w_v}{d+w_v+r_v}$$

we have

$$\begin{aligned} \frac{d\mathcal{F}_0}{dt} &\leq \left[\alpha\frac{d+w_v}{d+w_v+r_v} + gr_s - (d+r_s) \right] \mathcal{L} + \left[\beta(1-\rho)\frac{d+w_v}{d+w_v+r_v} - (d+d_0+r_c)g \right] \mathcal{I} \\ &= \left[\beta(1-\rho)\alpha\frac{d+w_v}{d+w_v+r_v} + \frac{\beta(1-\rho)(d+w_v)}{(d+w_v+r_v)(d+d_0+r_c)}r_s - (d+r_s) \right] \mathcal{L}, \\ &\quad + \left[\beta(1-\rho)\frac{d+w_v}{d+w_v+r_v} - (d+d_0+r_c)\frac{\beta(1-\rho)(d+w_v)}{(d+w_v+r_v)(d+d_0+r_c)} \right] \mathcal{I} \\ &= (d+r_s) \left[\frac{\beta(1-\rho)(d+w_v)(r_s + \alpha(d+d_0+r_c))}{(d+r_s)(d+w_v+r_v)(d+d_0+r_c)} - 1 \right] \mathcal{L} \\ &= (d+r_s)[\mathcal{R}_0 - 1]\mathcal{L}. \end{aligned}$$

If $\mathcal{R}_0 < 1$, Then $\frac{d\mathcal{F}_0}{dt} < 0$. Therefore, by LaSalle's Invariance Principle, it follows that the disease-free equilibrium point is globally asymptotically stable in Ω . \square

The following Theorem investigates the global dynamics of The endemic equilibrium, \mathcal{P}^* , of the COVID-19 epidemic model described in (1).

Theorem 3.5. *The endemic equilibrium point is globally asymptotically stable if $\mathcal{R}_0 > 1$.*

Proof. The appropriate Lyapunov function is defined as

$$\mathcal{F}^*(\mathcal{S}, \mathcal{L}, \mathcal{I}, \mathcal{V}, \mathcal{R}) = (m_1\mathcal{V}_* - m_2\mathcal{L}_*) \ln \left(\frac{\mathcal{S} + \mathcal{V}}{\mathcal{S}_* + \mathcal{V}_*} \right) - (\mathcal{L}_* + \mathcal{I}_* + \mathcal{R}_*) \ln \left(\frac{\mathcal{L} + \mathcal{I} + \mathcal{R}}{\mathcal{L}_* + \mathcal{I}_* + \mathcal{R}_*} \right),$$

where

$$m_1 = \frac{(d+r_s)(d+w_v+r_v)}{r_v}, \quad m_2 = \frac{\beta(1-\rho)(r_s + \alpha(d+d_0+r_c))}{d+d_0+r_c}.$$

Therefore

$$\frac{d\mathcal{F}^*}{dt} = \frac{(m_1\mathcal{V}_* - m_2\mathcal{S}_*)}{\mathcal{S} + \mathcal{V}} \left(\frac{d\mathcal{S}}{dt} + \frac{d\mathcal{V}}{dt} \right) - \frac{\mathcal{L}_* + \mathcal{I}_* + \mathcal{R}_*}{\mathcal{L} + \mathcal{I} + \mathcal{R}} \left(\frac{d\mathcal{L}}{dt} + \frac{d\mathcal{I}}{dt} + \frac{d\mathcal{R}}{dt} \right).$$

From (6), we have

$$(8) \quad m_1\mathcal{V}_* - m_2\mathcal{S}_* = \frac{\Lambda(d+r_s)M_2(1-\mathcal{R}_0)}{(\mathcal{R}_0-1)M_1+dM_2} \text{ and } \mathcal{L}_* + \mathcal{I}_* + \mathcal{R}_* = \frac{\Lambda M_2(\mathcal{R}_0-1)}{(\mathcal{R}_0-1)M_1+dM_2}.$$

by using the system (1) and the fact that $\mathcal{S}(t), \mathcal{L}(t), \mathcal{I}(t), \mathcal{V}(t), \mathcal{R}(t)$ are all non-negative for $t > 0$, we get

$$(9) \quad \frac{d\mathcal{S}}{dt} + \frac{d\mathcal{V}}{dt} \leq \Lambda + l_m\mathcal{R} \text{ and } \frac{d\mathcal{L}}{dt} + \frac{d\mathcal{I}}{dt} + \frac{d\mathcal{R}}{dt} \leq \beta(1-\rho)(\mathcal{I} + \alpha\mathcal{L}).$$

From (8) and (9), we have

$$\frac{d\mathcal{F}^*}{dt} \leq \frac{\Lambda M_2(1-\mathcal{R}_0)}{(\mathcal{R}_0-1)M_1+dM_2} \left(\frac{d+r_s}{\mathcal{S} + \mathcal{V}} (\Lambda + l_m\mathcal{R}) + \frac{1}{\mathcal{L} + \mathcal{I} + \mathcal{R}} (\beta(1-\rho)(\mathcal{I} + \alpha\mathcal{L})) \right).$$

If $\mathcal{R}_0 > 1$, we have $\frac{d\mathcal{F}^*}{dt} < 0$. Therefore, according to LaSalle's Invariance Principle, the endemic equilibrium point \mathcal{P}^* is globally asymptotically stable in Ω . \square

4. NUMERICAL SIMULATIONS

In this section, we will perform some numerical simulations in order to check the impact of quarantine and vaccination measures in controlling the spread of the COVID-19. Fig. 2 show the evolution of the exposed and infected individuals for the following parameters: $\Lambda = 8939$, $\beta = 0.4114$, $\alpha = 0.3131$, $d = 1/(67.7 * 365)$, $r_s = 0.0164$, $d_0 = 0.022$, $w_v = 0.0057$, $r_c = 0.1$, $l_m = 0.1762$. In the first case, we ignore the effect of quarantine and take the vaccination baseline, $\rho = 0$, $r_v = 0.0380$, the disease persist and the exposed and infected cases reach a very high level (the blue curve). In the second case, we increase the vaccination rate r_v by 50 percent from the baseline value, $\rho = 0$, $r_v = 0.057$, we can see that the disease persists with a significant reduction in both exposed and infected individuals (the red curve). Furthermore, in the third and the fourth cases, when the quarantine is maximally implemented simultaneously with population vaccination, the disease dies out and the infected, as well as exposed population, decreases very quickly (the yellow and purple curves).

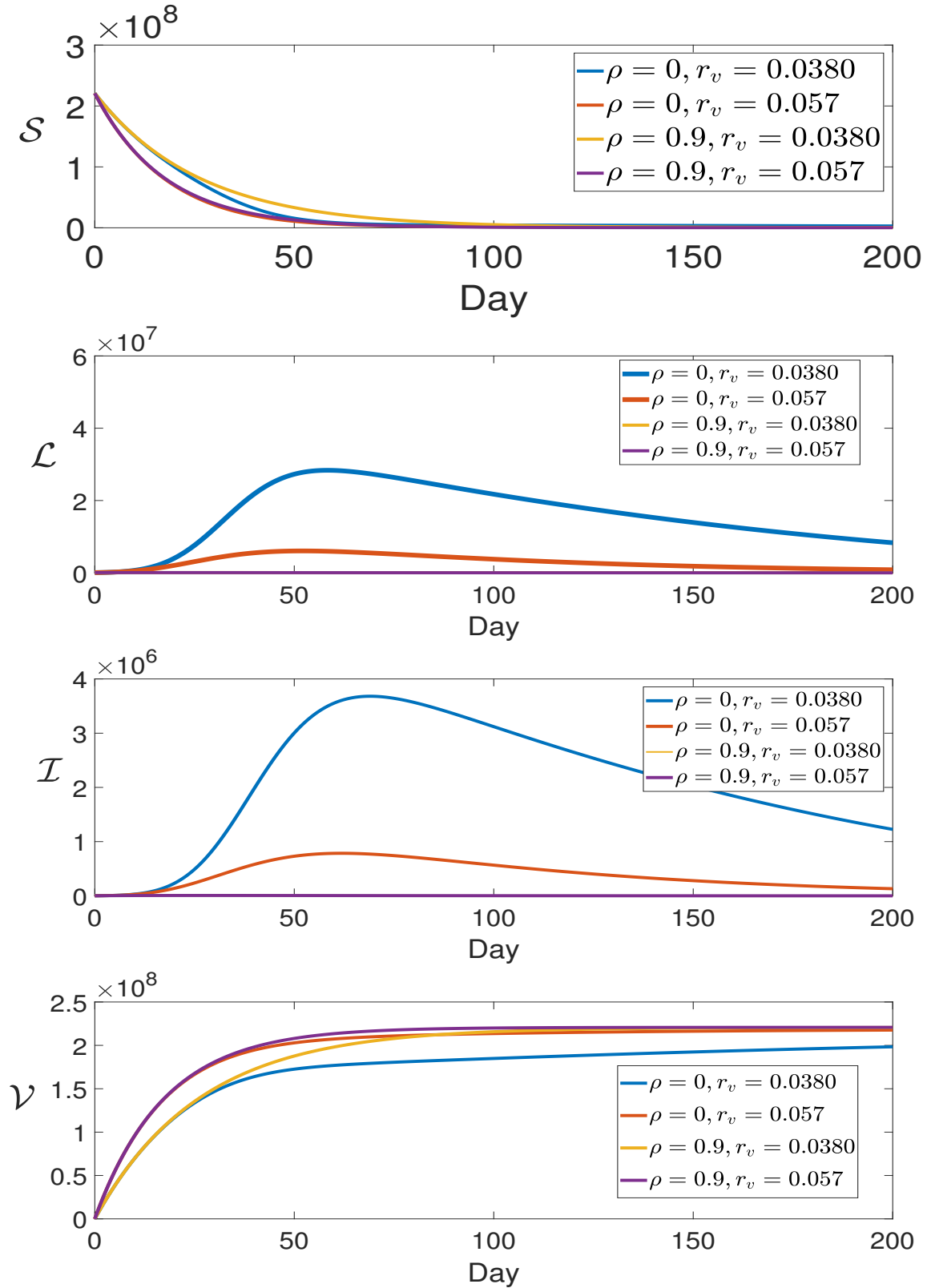


FIGURE 2. Impact of quarantine and vaccination strategies on exposed and infected population.

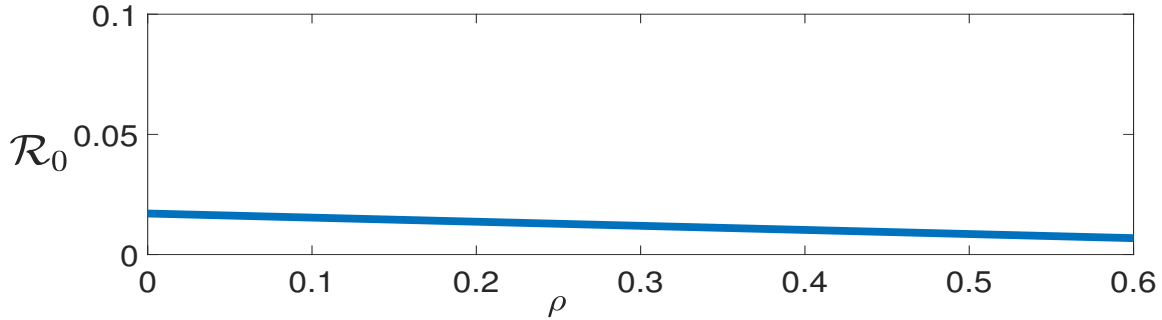


FIGURE 3. The figure on the left illustrates the variation of the basic reproduction number \mathcal{R}_0 as a function of the quarantine efficacy ρ in the absence of a vaccination strategy, while the figure on the right represents the variation the basic reproduction number \mathcal{R}_0 as a function of quarantine efficacy ρ when the vaccination strategy is considered.

The basic reproduction number \mathcal{R}_0 is affected by the quarantine effectiveness parameter and can be reduced by increasing quarantine efficacy. As a result, the quarantine strategy is critical in controlling COVID-19 disease. The critical value of quarantine effectiveness in the absence of vaccination of the population is estimated from Fig. (3) by 0.95, which means that the disease can converge to a disease-free state after more than 95 percent of the quarantine. However, when the vaccination strategy is considered, the critical value of quarantine efficiency is estimated from Fig. (3) by 0.31, signifying that the disease can converge to a disease-free state with only more than 31 percent of quarantine in the presence of vaccination.

5. CONCLUSION

In this paper, we have studied the mathematical model illustrating the dynamics of the COVID-19 disease with both vaccination and quarantine strategies. This model includes five equations describing the interaction between susceptible, exposed, infected, vaccinated, and recovered individuals. This study is oriented primarily toward to verify the positiveness and the boundedness of solutions that are established to have the well-posedness of the formulation. Furthermore, we have studied the existence and the stability of both disease-free equilibrium and endemic equilibrium, the Disease-free equilibrium always exists, and it is stable when

$\mathcal{R}_0 < 1$ but for the endemic equilibrium point exists and is stable when $\mathcal{R}_0 > 1$. Finally, the numerical simulations are carried out in order to show the behavior of the infection over time and to proclaim the effect of the quarantine and vaccination on both the COVID-19 dynamics and the basic reproduction number \mathcal{R}_0 for controlling the spread of the disease. We have concluded that the combination of quarantine and vaccination policies is the key aspect of infection control related to the spread of the COVID-19 outbreak.

CONFLICT OF INTERESTS

The authors declare that there is no conflict of interests.

REFERENCES

- [1] S. Amine, Y. Hajri, K. Allali, A delayed fractional-order tumor virotherapy model: Stability and Hopf bifurcation, *Chaos Solitons Fractals*. 161 (2022), 112396. <https://doi.org/10.1016/j.chaos.2022.112396>.
- [2] S. Amine, E.M. Farah, Global stability of HIV-1 and HIV-2 model with drug resistance compartment, *Commun. Math. Biol. Neurosci.* 2021 (2021), 38. <https://doi.org/10.28919/cmbn/5643>.
- [3] E.M. Farah, S. Amine, S. Ahmad, et al. Theoretical and numerical results of a stochastic model describing resistance and non-resistance strains of influenza, *Eur. Phys. J. Plus.* 137 (2022), 1169. <https://doi.org/10.1140/epjp/s13360-022-03302-5>.
- [4] Adnan, S. Ahmad, A. Ullah, et al. Complex dynamics of multi strain TB model under nonlocal and nonsingular fractal fractional operator, *Results Phys.* 30 (2021), 104823. <https://doi.org/10.1016/j.rinp.2021.104823>.
- [5] Z. Yaagoub, K. Allali, Fractional HBV infection model with both cell-to-cell and virus-to-cell transmissions and adaptive immunity, *Chaos Solitons Fractals*. 165 (2022), 112855. <https://doi.org/10.1016/j.chaos.2022.112855>.
- [6] A. Din, S. Amine, A. Allali, A stochastically perturbed co-infection epidemic model for COVID-19 and hepatitis B virus, *Nonlinear Dyn.* 111 (2022), 1921-1945. <https://doi.org/10.1007/s11071-022-07899-1>.
- [7] E.M. Farah, S. Amine, K. Allali, Dynamics of a time-delayed two-strain epidemic model with general incidence rates, *Chaos Solitons Fractals*. 153 (2021), 111527. <https://doi.org/10.1016/j.chaos.2021.111527>.
- [8] A. Allali, S. Amine, Stability analysis of a fractional-order two-strain epidemic model with general incidence rates, *Commun. Math. Biol. Neurosci.* 2022 (2022), 43. <https://doi.org/10.28919/cmbn/7297>.
- [9] D. Bentaleb, S. Amine, Lyapunov function and global stability for a two-strain SEIR model with bilinear and non-monotone incidence, *Int. J. Biomath.* 12 (2019), 1950021. <https://doi.org/10.1142/s1793524519500219>.
- [10] Z. Yaagoub, J. Danane, K. Allali, On a two-strain epidemic mathematical model with vaccination, *Computer Methods Biomech. Biomed. Eng.* (2023), 1-19. <https://doi.org/10.1080/10255842.2023.2197542>.

- [11] J. Nainggolan, J. Harianto, H. Tasman, An optimal control of prevention and treatment of COVID-19 spread in Indonesia, *Commun. Math. Biol. Neurosci.* 2023 (2023), 3. <https://doi.org/10.28919/cmbn/7820>.
- [12] S. Ahmad, A. Ullah, Q.M. Al-Mdallal, et al. Fractional order mathematical modeling of COVID-19 transmission, *Chaos Solitons Fractals.* 139 (2020), 110256. <https://doi.org/10.1016/j.chaos.2020.110256>.
- [13] K.S. Nisar, S. Ahmad, A. Ullah, et al. Mathematical analysis of SIRD model of COVID-19 with Caputo fractional derivative based on real data, *Results Phys.* 21 (2021), 103772. <https://doi.org/10.1016/j.rinp.2020.103772>.
- [14] I. Cooper, A. Mondal, C.G. Antonopoulos, A SIR model assumption for the spread of COVID-19 in different communities, *Chaos Solitons Fractals.* 139 (2020), 110057. <https://doi.org/10.1016/j.chaos.2020.110057>.
- [15] S.A. Lauer, K.H. Grantz, Q. Bi, et al. The incubation period of coronavirus disease 2019 (COVID-19) from publicly reported confirmed cases: estimation and application, *Ann. Internal Med.* 172 (2020), 577-582. <https://doi.org/10.7326/m20-0504>.
- [16] G. Pandey, P. Chaudhary, R. Gupta, et al. SEIR and regression model based COVID-19 outbreak predictions in India, *arXiv:2004.00958* (2020). <http://arxiv.org/abs/2004.00958>.
- [17] S. Rezapour, H. Mohammadi, M.E. Samei, SEIR epidemic model for COVID-19 transmission by Caputo derivative of fractional order, *Adv. Differ. Equ.* 2020 (2020), 490. <https://doi.org/10.1186/s13662-020-02952-y>.
- [18] Z. Yang, Z. Zeng, K. Wang, et al. Modified SEIR and AI prediction of the epidemics trend of COVID-19 in China under public health interventions, *J. Thorac. Dis.* 12 (2020), 165-174. <https://doi.org/10.21037/jtd.2020.02.64>.
- [19] S. He, Y. Peng, K. Sun, SEIR modeling of the COVID-19 and its dynamics, *Nonlinear Dyn.* 101 (2020), 1667-1680. <https://doi.org/10.1007/s11071-020-05743-y>.
- [20] S. Mwalili, M. Kimathi, V. Ojiambo, et al. SEIR model for COVID-19 dynamics incorporating the environment and social distancing, *BMC Res. Notes.* 13 (2020), 352. <https://doi.org/10.1186/s13104-020-05192-1>.
- [21] S. Annas, M.I. Pratama, M. Rifandi, et al. Stability analysis and numerical simulation of SEIR model for pandemic COVID-19 spread in Indonesia, *Chaos Solitons Fractals.* 139 (2020), 110072. <https://doi.org/10.1016/j.chaos.2020.110072>.
- [22] M. Amouch, N. Karim, Modeling the dynamic of COVID-19 with different types of transmissions, *Chaos Solitons Fractals.* 150 (2021), 111188. <https://doi.org/10.1016/j.chaos.2021.111188>.
- [23] A.A. Khan, S. Ullah, R. Amin, Optimal control analysis of COVID-19 vaccine epidemic model: a case study, *Eur. Phys. J. Plus.* 137 (2022), 156. <https://doi.org/10.1140/epjp/s13360-022-02365-8>.
- [24] O. Diekmann, J.A.P. Heesterbeek, J.A.J. Metz, On the definition and the computation of the basic reproduction ratio R_0 in models for infectious diseases in heterogeneous populations, *J. Math. Biol.* 28 (1990), 365-382. <https://doi.org/10.1007/bf00178324>.